CONSTRAINTS ON THE MASS ACCRETION RATE OF NEUTRINO-COOLED DISKS IN GAMMA-RAY BURSTS

Tong Liu, Wei-Min Gu, Li Xue, Shan-Shan Weng, and Ju-Fu Lu*

Department of Physics and Institute of Theoretical Physics and Astrophysics, Xiamen University, Xiamen, Fujian 361005, China

*lujf@xmu.edu.cn

ABSTRACT

We present a unified description of all the three known classes of optically thick accretion disks around black holes, namely Shakura-Sunyaev disks, slim disks, and neutrino-dominated accretion flows (NDAFs). It is found that NDAFs have both a maximal and a minimal possible mass accretion rate at their each radius. This may be suggestive of an interpretation for the origin of X-ray flares observed in gamma-ray bursts.

Subject headings: accretion, accretion disks - black hole physics - gamma rays: bursts - neutrinos

1. Introduction

Recently, Gu & Lu (2007) addressed a theoretical problem regarding the slim accretion disk model in the fundamental sense. In this model (e.g., Abramowicz et al. 1988; Kato et al. 1998, p.242), in dealing with the vertical hydrostatic equilibrium of the disk, the well-known pseudo-Newtonian potential of Paczyński & Wiita (1980),

$$\psi(r,z)=-\frac{GM}{\sqrt{r^2+z^2}-r_{\rm g}}, \tag{1}$$

was approximated in the form suggested by Hōshi (1977), i.e.,

$$\psi(r,z)=\psi(r,0)+\Omega_{\rm K}^2 z^2/2, \tag{2}$$

where r and z are cylindrical coordinates, M is the mass of the central black hole, $r_{\rm g}\equiv 2GM/c^2$ is the Schwarzschild radius, and $\Omega_{\rm K}=(GM/r)^{1/2}/(r-r_{\rm g})$ is the Keplerian angular velocity. As shown by Gu & Lu (2007), equation (2) is valid only for geometrically thin

disks such as Shakura-Sunyaev disks (SSDs, Shakura & Sunyaev 1973), i.e., with $H \ll r$, where H is the half-thickness of the disk; and this equation is invalid for slim disks that may have $H \lesssim r$ or $H \sim r$, because in this case it would greatly magnify the gravitational force in the vertical direction of the disk, $\partial\psi/\partial z$. When the explicit form of Paczyński-Wiita potential, equation (1), is used to calculate the vertical gravitational force, the relationship that is obtained with equation (2) and is applicable only for geometrically thin disks, i.e., $c_{\rm s}/\Omega_{\rm K}H =$ constant, where $c_{\rm s}$ is the sound speed, does not hold for slim disks. Accordingly and more seriously, it is found that slim disks cannot exist at large radii of black hole accretion flows with large accretion rates, and only the inner regions of these flows can possibly take the form of slim disks provided accretion rates are effectively reduced by outflows from the outer regions.

Slim disk are optically very thick in the vertical direction, such that photons are sufficiently trapped within the disk and advected along with the disk matter into the black hole. In this paper, we extend the work of Gu & Lu (2007) into another class of accretion disks, namely neutrino-cooled accretion disks (or neutrino-dominated accretion flows, NDAFs) around stellar-mass black holes. These disks are known to be plausible candidates for the central engines of gamma-ray bursts (Popham et al. 1999; Narayan et al. 2001; Kohri & Mineshige 2002; Di Matteo et al. 2002; Kohri et al. 2005; Lee et al. 2005; Gu et al. 2006; Chen & Beloborodov 2007; Liu et al. 2007; Kawanaka & Mineshige 2007; Janiuk et al. 2007). They can be regarded as an even more extreme case of optically thick disks, since their density and temperature are so high ($\rho \sim 10^{10}$g cm^{-3}, $T \sim 10^{10}$K) that photons are completely trapped and only energetic neutrinos are emitted away.

2. Equations

NDAFs may have H comparable to r (e.g., Popham et al. 1999; Chen & Beloborodov 2007; Janiuk et al. 2007), so their hydrodynamics and thermodynamics are expected to be similar to those of slim disks. We write the continuity, radial momentum, angular momentum, and energy equations of NDAFs in the formalism of Gu & Lu (2007) for slim disks, where equation (1) was used to integrate the vertical hydrostatic equilibrium equation and the simple relation $c_{\rm s}/\Omega_{\rm K}H =$ constant was abandoned:

$$\dot{M} = -2\pi r\Sigma v_r = \text{constant} \ , \tag{3}$$

$$v_r\frac{{\rm d}v_r}{{\rm dln}r} + c_{\rm s}^2\frac{{\rm dln}\Pi}{{\rm dln}r} - \Omega^2 r^2 = -\frac{\Omega_{\rm K}^2(r-r_{\rm g})^2}{\Sigma}\int_{-H}^{H}\frac{\rho}{[\sqrt{1+(z/r)^2}-r_{\rm g}/r]^2\sqrt{1+(z/r)^2}}{\rm d}z \ , \tag{4}$$

$$\dot{M}(\Omega r^2 - j_0) = 2\pi\alpha r^2\Pi \ , \tag{5}$$

$$Q_{\rm vis} = Q_{\rm adv} + Q_{\nu} \ . \tag{6}$$

In these equations, $\dot{M}$ is the mass accretion rate, v_r is the radial velocity, Ω is the angular velocity, $\Sigma = \int_{-H}^{H} \rho {\rm d}z$ is the surface density, $\Pi = \int_{-H}^{H} p {\rm d}z$ is the vertically integrated pressure, ρ is the mass density, p is the pressure, the sound speed is defined as $c_{\rm s} = (\Pi/\Sigma)^{1/2}$, j_0 is an integration constant representing the specific angular momentum accreted by the black hole, and α is the Shakura-Sunyaev viscosity parameter. The viscous heating rate is $Q_{\rm vis} = \dot{M}\Omega^2 f g/2\pi$, where $f = 1 - j/\Omega_{\rm K} r^2$, $j = j_0/\omega$, $\omega = \Omega/\Omega_{\rm K}$ is assumed to be a constant that is smaller than 1 (sub-Keplerian rotation), and $g = -{\rm dln}\Omega_{\rm K}/{\rm dln}r$; the advective cooling rate is $Q_{\rm adv} = \xi \dot{M} {c_{\rm s}}^2/2\pi r^2$, with ξ being a dimensionless quantity of the order of unity (Kato et al. 1998, p.272). All these definitions and relations are similar to those for slim disks. What is new in the case of NDAFs, however, is that in the energy equation (6) there is a cooling term due to neutrino radiation, Q_{ν}, instead of the cooling term due to photon radiation, $Q_{\rm rad}$, because of the photon trapping. The neutrino cooling is expressed by a bridging formula that is valid in both the neutrino optically thin and thick regimes:

$$Q_{\nu} = \sum_i \frac{(7/8)\sigma T^4}{(3/4)[\tau_{\nu_i}/2 + 1/\sqrt{3} + 1/(3\tau_{a,\nu_i})]} \tag{7}$$

(Korhi et al. 2005), where T is the temperature, τ_{ν_i} is the total optical depth for neutrinos, τ_{a,ν_i} is the absorption optical depth for neutrinos, and the subscript i runs over the three species of neutrinos $\nu_{\rm e}$, ν_{μ} , and ν_{τ} (see, e.g., Kohri et al. [2005] and Liu et al. [2007] for detailed analyses and calculations of these optical depths). Accordingly, the equation of state is also different from that for slim disks, it is written as

$$p = p_{\rm gas} + p_{\rm rad} + p_{\rm e} + p_{\nu}, \tag{8}$$

where $p_{\rm gas}$, $p_{\rm rad}$, $p_{\rm e}$, and p_{ν} are the gas pressure from nucleons, radiation pressure of photons, degeneracy pressure of electrons, and radiation pressure of neutrinos, respectively. Of these four pressure components, there are only the first two for slim disks, while the last two are newly appeared for NDAFs. Detailed expressions for these four components are also given in, e.g., Kohri et al. (2005) and Liu et al. (2007). An additional note about the energy equation (6) is that, for simplicity, we ignore another cooling term due to photodisintegration of α-particles and other heavier nuclei; in other words, we assume that in NDAFs all heavy nuclei are already disintegrated into nucleons.

3. Unified Description of SSDs, Slim Disks, and NDAFs

With the procedure similar to that of Gu & Lu (2007), thermal equilibrium solutions at a certain radius can be obtained from equations (3) - (6) and (8), with given constant

parameters M, $\dot{M}$, α, and j. In our calculations we take $M = 3M_{\odot}$, $\alpha = 0.1$, and $j = 1.83cr_{\rm g}$.

As our main result, Figure 1 shows thermal equilibria of NDAFs at each radius r with corresponding accretion rates $\dot{M}$. The left and right vertical axes are for $\dot{M}$ in units of the Eddington accretion rate $\dot{M}_{\rm Edd} = 64\pi GM/c\kappa_{\rm es}$, where $\kappa_{\rm es} = 0.34{\rm cm}^2{\rm g}^{-1}$ is the electron scattering opacity, and of $M_{\odot}$ s^{-1} , respectively. To have a complete picture of all the known classes of optically thick accretion disks around black holes, the results of Gu & Lu (2007) for SSDs and slim disks are also included in the figure. It is seen that the $\dot{M}$-r plane is divided into four regions by five lines a, b, c, d, and e. As described in Gu & Lu (2007), the region below line a is for stable, photon radiation-cooled and gas pressure-supported SSDs; the region between lines a and b is for unstable, photon radiation pressure-supported but not yet advective cooling-dominated SSDs; the region between lines b and c is for stable, advective cooling-dominated and photon radiation pressure-supported slim disks; and line c represents a maximal possible accretion rate for each radius, above which no thermal equilibrium solutions exist because the viscous heating $Q_{\rm vis}$ is always larger than the total cooling ($Q_{\rm adv} + Q_{\rm rad}$). What is new in the figure is lines d and e. The 'no solution' region above line c extends upward till line d, above which the cooling due to neutrino radiation, Q_{ν}, becomes important or even dominant, such that thermal equilibrium solutions can be established again, and these are exactly NDAF solutions. Thus, line d represents the lower limit of $\dot{M}$ needed for NDAFs to be realized. Similar to line c, line e shows the upper limit of $\dot{M}$ for NDAFs, beyond which the heating $Q_{\rm vis}$ is always too large to be balanced by the total cooling ($Q_{\rm adv} + Q_{\nu}$), and no thermal equilibrium solutions can exist. Therefore, the joining point of lines d and e at $r \approx 185r_{\rm g}$, marked by a filled circle, defines the maximal possible outer boundary of an NDAF. We repeat that the finding of a radius-dependent maximal possible accretion rate, $\dot{M}_{\rm max}(r)$, for slim disks as well as for NDAFs (i.e., lines c and e) is because of the usage of equation (1). The physical reason for the existence of $\dot{M}_{\rm max}(r)$ is that the black hole's gravitational force in the vertical direction, correctly calculated from equation (1), can only gather some limited amount of accreted matter; beyond this limit the pressure force would be too large to be balanced by the gravitational force, and outflows are likely to be produced as a result.

Note that in Figure 1 the upper limit line c for slim disks and the lower limit line d for NDAFs join into a single line at $r \approx 18.6r_{\rm g}$, and the region for slim disk solutions and that for NDAF solutions combine into a single region, ranging over several orders of magnitude in $\dot{M}$. There is no boundary separating these two seemingly very different classes of black hole accretion disks, slim disks and NDAFs. Both of them are optically very thick for photons. As the accretion rate increases, the processes of neutrino emission operate and become important, and the accretion flow changes from the slim disk form to the NDAF form. By also including SSD solutions, which are separated from slim disk solutions by the

unstable region and can possibly connect slim disk solutions via limit-cycle oscillations (e.g., Szuszkiewicz & Miller 2001; Li et al. 2007), Figure 1 does provide a unified description of all the three known classes of optically thick accretion disks around black holes.

Line e in Figure 1 looks to indicate that for very small radii, the allowed accretion rate of NDAFs could be as high as $\sim 10^5 - 10^6 M_\odot \mathrm{s}^{-1}$. One might worry that the density of the flow matter there could reach up to the same as or even larger than the nuclear density, then there would be uncertainties in calculating the total pressure, the neutrino cooling rate and so on, because such calculations need information about the nuclear equation of state in detail which is highly model-dependent and unclear at present. Our answer to this problem is that such a high accretion rate for a small radius is only a theoretical upper limit and is unlikely to be astrophysically realizable. All the related theoretical models and numerical calculations have agreed that the accretion rate needed to power a GRB is in the range of $\sim 0.01 - 10 M_\odot \mathrm{s}^{-1}$ (e.g., Popham et al. 1999; Kawanaka & Mineshige 2007). We plot in Figure 2 the mass density on the equatorial plane, ρ_0, as functions of r for four different values of $\dot{M}$: 0.01, 0.1, 1, and $10 M_\odot \mathrm{s}^{-1}$. It is seen that even for $\dot{M} = 10 M_\odot \mathrm{s}^{-1}$, ρ_0 is far below the nuclear density which is $\sim 10^{14} \mathrm{g\ cm}^{-3}$. Our calculations also give that (not drawn in Figure 2) only for an (unrealistically) high accretion rate $\dot{M} \sim 10^6 M_\odot \mathrm{s}^{-1}$, ρ_0 could reach up to $\sim 10^{14} \mathrm{g\ cm}^{-3}$ in a very small region $r \lesssim 4 r_\mathrm{g}$. Thus, Figure 1 does not seem to suffer the density problem.

Figure 3 shows thermal equilibrium solutions in the $\dot{M}$-Σ plane for fixed radii $r = 5 r_\mathrm{g}$ (the solid line) and $r = 100 r_\mathrm{g}$ (the dashed line). Such a design is widely found in the literature as it is a useful tool for the local stability analysis: solutions on the lines with a positive derivative ($\partial \dot{M} / \partial \Sigma > 0$) are viscously stable, while those with a negative derivative ($\partial \dot{M} / \partial \Sigma < 0$) are viscously unstable (e.g., Kato et al. 1998). As seen from the figure, for a small radius ($r = 5 r_\mathrm{g}$) there is a continuous S-shaped sequence of thermal equilibria, of which the lower and middle branches correspond to stable SSDs and unstable SSDs, respectively; and the upper branch extends from stable slim disk solutions to stable NDAF solutions with increasing $\dot{M}$ and ends at the maximal possible $\dot{M}$ for NDAFs (i.e., line e in Fig. 1). For a large radius ($r = 100 r_\mathrm{g}$), however, the solution sequence is no more continuous and is broken into two parts by the 'no solution' region shown in Figure 1: the lower part is still for stable SSDs and unstable SSDs, and the upper part is for stable NDAFs and is bounded by the minimal and maximal possible $\dot{M}$(i.e., lines d and e in Fig. 1). Previous works (Kohri & Mineshige 2002; Di Matteo et al. 2002; Kawanaka & Mineshige 2007) have proved that NDAFs are stable. Our results here confirm this conclusion, but with an additional remark that for NDAFs the allowed accretion rate has both a lower and an upper limit.

All the above results are obtained with a one-dimensional (1-D) analytical model, that

is, as in most previous works on slim disks as well as NDAFs (see the references in §1), we solve the vertically integrated equations and do not consider the vertical structure of the disk. Strictly speaking, simple 1-D models can be valid only for geometrically thin disks such as SSDs. For slim disks and NDAFs which are geometrically not thin, the multidimensional effects on the disk's basic properties, e.g., the various timescales and the cooling rates can be important or even crucial, so the validity of 1-D approximations should be checked by at least two-dimensional (2-D) studies. Recently, 2-D radiation-hydrodynamical numerical simulations and analytical treatments of supercritical accretion flows, to which slim disks and NDAFs belong, have been made (Ohsuga et al. 2005; Ohsuga 2007; Kohri et al. 2007). These works showed that it is indeed quite important to consider carefully the vertical dependence of fluid quantities and the radiative diffusion in the vertical direction. Compared with the correct 2-D results, the 1-D slim disk model (Abramowicz et al. 1988; Kato et al. 1998) tends to overestimate $Q_{\rm rad}$, and hence, underestimate $Q_{\rm adv}$ and overestimate the luminosity. Another important multidimensional effect for slim disks is that photon trapping modifies the spectral energy distribution. For NDAFs, however, similar multidimensional effects were only predicted but not proved (Kohri et al. 2007). Having mentioned these recent 2-D works, we think that the validity of our 1-D results here is unlikely to be affected. We do not calculate the luminosity or the radiation spectrum. What we have done is a dynamical study. We pay attention to the thermal equilibrium between the viscous heating $Q_{\rm vis}$ and the total cooling, which is the sum of $Q_{\rm rad}$ and $Q_{\rm adv}$ for slim disks and the sum of Q_ν and $Q_{\rm adv}$ for NDAFs. Even though $Q_{\rm rad}$ (and maybe Q_ν too) may be overestimated and $Q_{\rm adv}$ underestimated in the 1-D calculations, these two inaccuracies should tend to cancel with each other, such that the resulting total cooling is likely to remain a reasonable estimate. From the analysis of thermal equilibrium solutions we find, as our main result, that NDAFs have both a maximal and a minimal possible accretion rate at their each radius. This result implies that outflows driven by the pressure force are likely to originate from accretion flows with an accretion rate exceeding its allowed upper limit. Such outflows have been found in the 2-D simulations of supercritical accretion flows (Ohsuga 2007).

4. On the Origin of X-Ray Flares in Gamma-Ray Bursts

We discuss briefly an astrophysical implication of our results. A new, unexpected phenomenology of gamma-ray bursts (GRBs) revealed by the *Swift* satellite is erratic X-ray flares following a number of long-duration and short-duration GRBs. Such flares generally rise and fall rapidly, with typical time scales much shorter than the epoch when the flare occurs. This time behavior strongly supports the 'internal' origin of the flares, in contrast to the 'external' origin of the power-law decay afterglows; that is, it indicates a restart of

the GRB central engine (see, e.g., Proga & Zhang [2006] for references). Although long and short GRBs are likely to be associated with different types of progenitors, namely collapsars for long GRBs and mergers of compact objects for short ones; it is generally believed that the central engines of these two classes of events are in common invoking a hyperaccretion disk around a stellar-mass black hole (see, e.g., Perna et al. [2006] for references). Thus, a restart of the GRB central engine is just a restart of accretion. Based on these considerations, models for a common origin of the X-ray flares in both long and short GRBs have been recently proposed, in which accretion of a black hole is repeatedly ended and then restarted either by the fragmentation in the outer parts of accretion flows (Perna et al. 2006), or by the magnetic flux accumulated in the vicinity of the black hole (Proga & Zhang 2006).

Taking the view that hyperaccretion disks radiate their gravitational energy as neutrinos to power GRBs (i.e., NDAFs, see references listed in §1), our results here may be suggestive of a new and simpler interpretation for the cause of ending and restarting the accretion process. As seen from Figure 1, NDAF solutions can exist only for the region bounded by lines d and e, the joining point (the filled circle) of these two limit lines defines the largest possible outer boundary, $r^* \approx 185 r_{\rm g}$, of an NDAF and corresponds to an accretion rate $\dot{M}^* \approx 0.62 M_\odot {\rm s}^{-1}$. Thus, depending on the place where an inflow toward the black hole originally starts and the available mass supply rate, there are following three distinct cases. (1) The inflow starts at a radius $r < r^*$ and the mass supply rate is within the region between lines d and e. In this case, an NDAF forms and a GRB appears, but no flares follow. (2) The inflow either starts at $r < r^*$ with a mass supply rate below line d, or starts at $r > r^*$ with a mass supply rate less than $\dot{M}^*$. This is the case in which no NDAFs can form and no GRBs are produced at all. (3) The inflow either starts at $r < r^*$ with a mass supply rate above line e, or starts at $r > r^*$ with a mass supply rate larger than $\dot{M}^*$. In this case, the flow must first lose matter in the form of outflows (because the pressure force exceeds the gravitational force, as mentioned in §3), such that its remaining matter ensures an accretion rate within the region between lines d and e, then there is an NDAF and a GRB. This primary hyperaccretion ends when the matter in the NDAF is all swallowed by the central black hole as in case 1, but this is not all. Some or all of the outflowing matter can be attracted backward again by the black hole. It is this feedback that is responsible for restarting accretion. Such secondary accretion is expected to have a rate that is substantially lower than the primary hyperaccretion rate and is insufficient to support another NDAF, so it is likely to be in the form of photon radiation-cooled disks that produce X-ray flares. In this line, a detailed model for X-ray flares in GRBs is being worked out.

For the moment, let us add a few more words about the realistic initial conditions of hyperaccretion flows and the possibilities of the mechanism for X-ray flare production suggested here, by comparing the results for $\dot{M}$ and the outer boundary of NDAFs given

in Figure 1 with those existed in the literature. As already mentioned in §3, in all the known theoretical models and numerical calculations $\dot{M}$ needed to power a GRB is in the range of $\sim 0.01 - 10 M_{\odot}\mathrm{s}^{-1}$. Further, the most probable $\dot{M}$ for NDAFs is in the range of $\sim 0.2-1 M_{\odot}\mathrm{s}^{-1}$ (Kawanaka & Mineshige 2007). For the outer boundary of NDAFs, defined as the radius inside which neutrino cooling is significant, Chen & Beloborodov (2007) calculated that it is $\sim 100 r_{\mathrm{g}}$ for $\alpha = 0.1$ and $\sim 200 r_{\mathrm{g}}$ for $\alpha = 0.01$. All these values are consistent with the NDAF region bounded by lines d and e in Figure 1. Regarding the realistic conditions in the progenitor systems of GRBs, it is less clear where the inflow originally starts and how large the initial mass supply rate is, but it seems plausible that short GRBs resulted from mergers of compact objects have smaller accretion disks and long GRBs resulted from collapsars have larger ones (e.g., Popham et al. 1999; Narayan et al. 2001). In view of these facts, there should be possibilities for case 3 described above to be realized. For instance, if an inflow starts at $r < r^*$ with a mass supply rate above line e, then the resulting GRB is likely a short one with flares following it; or if an inflow starts at $r > r^*$ with a mass supply rate larger than $\dot{M}^*$, then it is the chance for a long GRB instead, and with flares too.

We thank Z. G. Dai for beneficial discussions and the referee for helpful comments. This work was supported by the National Natural Science Foundation of China under grants 10503003 and 10673009 and the Natural Science Foundation of Fujian Province of China under grant V0750001.

REFERENCES

Abramowicz, M. A., Czerny, B., Lasota, J.-P., & Szuszkiewicz, E. 1988, ApJ, 332, 646

Chen, W.-X., & Beloborodov, A. M. 2007, ApJ, 657, 383

Di Matteo, T., Perna, R., & Narayan, R. 2002, ApJ, 579, 706

Gu, W.-M., Liu, T., & Lu, J.-F. 2006, ApJ, 643, L87

Gu, W.-M., & Lu, J.-F. 2007, ApJ, 660, 541

Hōshi, R. 1977, Prog. Theor. Phys., 58, 1191

Janiuk, A., Yuan, Y.-F., Perna, R., & Di Matteo, T. 2007, ApJ, 664, 1011

Kato, S., Fukue, J., & Mineshige, S. 1998, Black-Hole Accretion Disks (Kyoto: Kyoto Univ. Press)

Kawanaka, N., & Mineshige,S. 2007, ApJ, 662, 1156

Kohri, K., & Mineshige, S. 2002, ApJ, 577, 311

Kohri, K., Narayan, R. & Piran, T. 2005, ApJ, 629, 341

Kohri, K., Ohsuga, K., & Narayan, R. 2007, MNRAS, 381, 1267

Lee, W. H., Ramirez-Ruiz, E., & Page, D. 2005, ApJ, 632, 421

Li, S.-L., Xue, L., & Lu, J.-F. 2007, ApJ, 666, 368

Liu, T., Gu, W.-M., Xue, L., & Lu J.-F. 2007, ApJ, 661, 1025

Narayan, R., Piran, T., & Kumar, P. 2001, ApJ, 557, 949

Ohsuga, K. 2007, ApJ, 659, 205

Ohsuga, K., Mori, M., Nakamoto, T., &Mineshige, M. 2005, ApJ, 628, 368

Paczyński, B., & Wiita, P. J. 1980, A&A, 88, 23

Perna, R., Armitage, P. J., & Zhang, B. 2006, ApJ, 636, L29

Popham, R., Woosley, S. E., & Fryer, C. 1999, ApJ, 518, 356

Proga, D., & Zhang, B. 2006, MNRAS, 370, L61

Shakura, N. I., & Sunyaev, R. A. 1973, A&A, 24, 337

Szuszkiewicz, E., & Miller, J. C. 2001, MNRAS, 328, 36

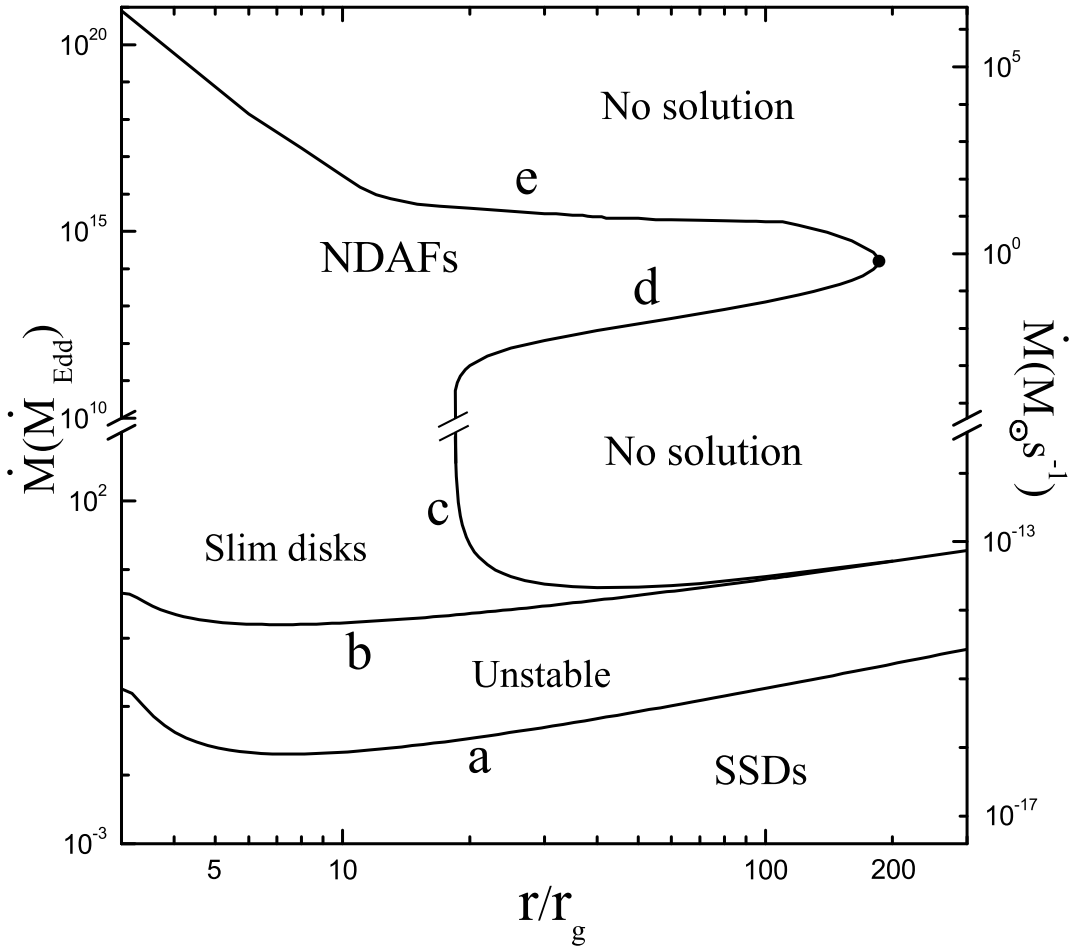

Fig. 1.— Distribution of black hole optically thick accretion disk solutions. The $\dot{M}$-r plane is divided into four regions by five boundary lines a, b, c, d, and e. The filled circle denotes the largest possible outer boundary of an NDAF.

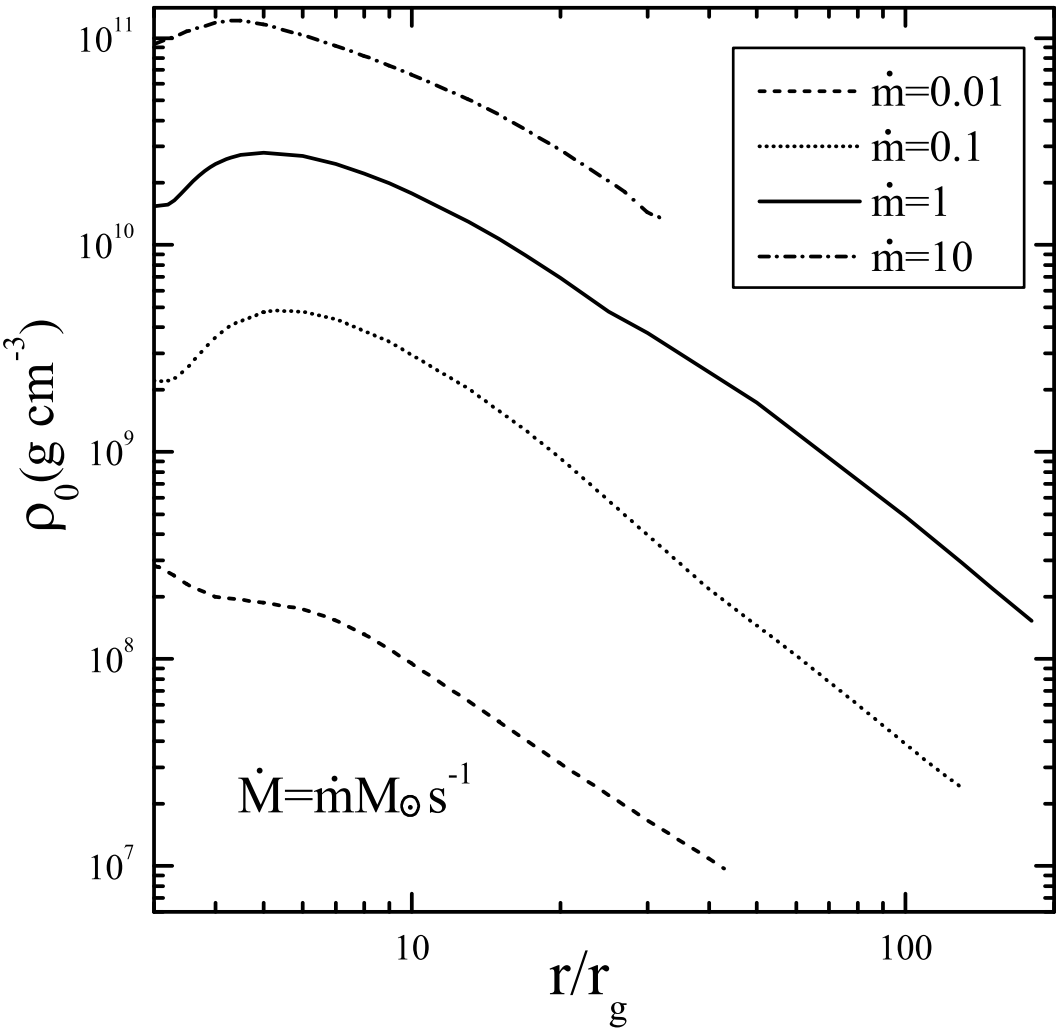

Fig. 2.— Radial dependence of the mass density ρ_0 of NDAFs for different possible values of $\dot{M}$: 0.01 (dashed line), 0.1 (dotted line), 1 (solid line), and 10 (dot-dashed line) $M_\odot \mathrm{s}^{-1}$.

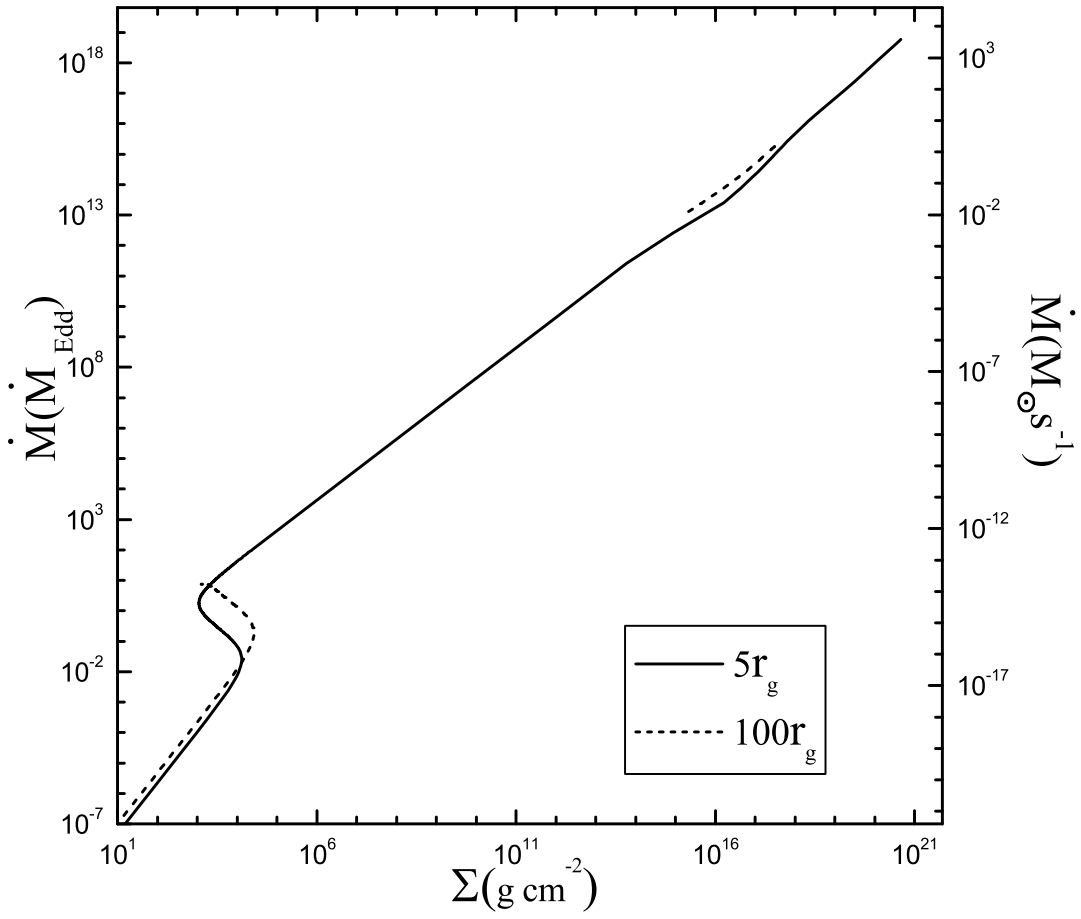

Fig. 3.— Stability curves in the $\dot{M}$-Σ plane for radii $5r_{\rm g}$ (solid line) and $100r_{\rm g}$ (dashed line).